

# Nonextensive statistics in viscous fingering

Patrick Grosfils, Jean Pierre Boon<sup>1</sup>

*Center for Nonlinear Phenomena and Complex Systems  
Université Libre de Bruxelles, 1050 - Bruxelles, Belgium*

---

## Abstract

Measurements in turbulent flows have revealed that the velocity field in nonequilibrium systems exhibits  $q$ -exponential or power law distributions in agreement with theoretical arguments based on nonextensive statistical mechanics. Here we consider Hele-Shaw flow as simulated by the Lattice Boltzmann method and find similar behavior from the analysis of velocity field measurements. For the transverse velocity, we obtain a spatial  $q$ -Gaussian profile and a power law velocity distribution over all measured decades. To explain these results, we suggest theoretical arguments based on Darcy's law combined with the non-linear advection-diffusion equation for the concentration field. Power law and  $q$ -exponential distributions are the signature of nonequilibrium systems with long-range interactions and/or long-time correlations, and therefore provide insight to the mechanism of the onset of fingering processes.

*PACS* : 47.20.Gv, 05.70.Ln, 05.10.-a

*Keywords* : Power law distribution; Nonextensive statistics; Hele-Shaw flow.

---

Experiments in turbulent flows (such as Couette-Taylor flow [1]) have shown that data obtained from quantities extracted from velocity field measurements in these nonequilibrium systems exhibit power law or  $q$ -exponential velocity distributions which have been analyzed and interpreted with theoretical arguments based on nonextensive statistical mechanics [2]. Other physical systems have been shown to exhibit similar type distributions as a consequence of *nonextensivity* [3]. Here we consider fingering which occurs in the interfacial zone between two fluids confined between two plates with a narrow gap (Hele-Shaw geometry) when one of the fluids is displaced by the other fluid, the interfacial instability resulting from mobility differences between the fluids. Using a mesoscopic approach - the lattice Boltzmann method - we investigated the dynamics of spatially extended Hele-Shaw flow [4]. We are primarily interested in the early stage of the fingering process in order to explore the characteristics of the velocity field after the destabilization of the interface.

---

<sup>1</sup> *E-mail address* : [jdboon@ulb.ac.be](mailto:jdboon@ulb.ac.be); *URL* : <http://poseidon.ulb.ac.be>

The Hele-Shaw geometry is intrinsically tri-dimensional, but the effective destabilization of the flow can be described in the 2-D plane, the flow being purely Poiseuille flow in the third dimension of the shallow layer [5]. So we can simulate Hele-Shaw flow by using the two-dimensional LBGK equation, the Bhatnagar-Gross-Krook version of the lattice Boltzmann equation where the full collision term is approximated by a single relaxation term [6]. One emulates 3-D flow by introducing a drag term, thereby simulating a system with a virtual cell gap in the third dimension: the drag enters the LBGK equation as a damping term [7].

As the simulation method has been described in detail in a previous publication [8], we merely outline the essentials of the physics of the problem as it is simulated. The system consists of a 2-D rectangular box with vertical length  $L_y$  and horizontal width  $L_x$  ( $L_x \times L_y = 1024 \times 2048$  nodes) filled with fluid 2 which is being displaced by fluid 1 injected uniformly from the top of the box (the respective drag coefficients are  $\beta_1 < \beta_2$ ). Fluid 1 invades the system through a constant drift applied along the  $y$ -direction. The initial concentration profile of fluid 1 is a step function which, because of mutual diffusion between the two miscible fluids, develops into an  $\text{erfc}$   $y$  profile. The interfacial profile which is initially flat along the transverse  $x$ -direction, is perturbed with white noise to trigger the instability. Any small perturbation so induced is the siege of a local pressure gradient normal to the interface where from the instability develops as illustrated in Fig.1.

Measurements of the time evolution of the mixing length ( $L_{mix}$ ) of the interfacial zone (see Fig.1) show a dynamical transition from the short time diffusive regime to the nonlinear regime [8]. The short time behavior obeys a power law  $L_{mix} \propto t^\mu$  with  $\mu \simeq 1/2$ ; then (as shown in Fig.3 in [8]) a transition is observed from the diffusive regime with the “early time exponent”  $1/2$  to the regime with a “dynamic exponent”  $\mu \simeq 2.3$ , a value which was obtained from lattice Boltzmann simulation as well as from direct numerical simulations of Darcy’s equation [8]. Here we shall restrict to the investigation of the transverse velocity field ( $v_x$ ), that is the field transverse to the propagation direction of the flow, during the onset of fingering. What is meant by *onset* is the late stage of the diffusive regime with  $\mu \simeq 1/2$  (see Fig.3 in [8]) where the fingers have developed into a regular pattern (see Fig.1) before growing into the competitive stage where large fingers absorb slower smaller fingers, a feature characteristic of the nonlinear regime with  $\mu \simeq 2.3$ .

When the planar interface destabilizes, the flow develops a wiggling concentration profile (in the  $x$ -direction) thereby producing local concentration gradients which trigger vorticity fluctuations. Pattern formation follows in the velocity field as shown in Fig.2a, and “vortices” are being created with alternating polarities. They are reminiscent of vortex patterns in two-dimensional turbulent flows, although here the Reynolds number has low value. However the

relevant control parameter, the Péclet number, is high:  $Pe = L_x |\mathbf{v}_y| / D \simeq 200$  ( $D$  is the diffusion coefficient). We performed measurements of the velocity field and found that the transverse component  $v_x$  in each vortex shows a  $q$ -Gaussian profile (see Fig.2b), and that the corresponding velocity distribution,  $P(v_x)$ , obtained by computing  $v_x$  over all vortices, follows a power law,  $P(v_x) \propto v_x^{-0.875}$  (see Fig.3).

It has been shown that processes stemming from the generalized Fokker-Planck equation [3,9,10] or the generalized advection-diffusion equation [11,12] can produce stationary solutions of the  $q$ -exponential type provided some conditions are met for the drift and dissipative functions. In the present simulations, we observe that the concentration field exhibits a  $q$ -Gaussian profile which suggests that the concentration  $C(x, t)$  is governed by the "porous media equation" [13]

$$\partial_t C(x, t) + \partial_x [K(x) C(x, t)] = \partial_x [D(x) \partial_x C^\alpha(x, t)], \quad (1)$$

where  $K(x)$  and  $D(x)$  are the drift and dissipation functions respectively. Note that the second term in (1) can be rewritten formally as

$$\partial_x [D \partial_x C^\alpha] = \partial_x [D_\alpha \partial_x C], \quad (2)$$

where  $D_\alpha = \alpha D_0 C^{\alpha-1}$ . The stationary solution to Eq.(1) is a  $q$ -exponential of the form (see e.g. [10])

$$C(x) = C_0 e_q^{-\gamma_q |x|^\lambda} = C_0 [1 - (1 - q)\gamma_q |x|^\lambda]^{\frac{1}{1-q}}, \quad (3)$$

where  $C_0$  is a normalization constant, and  $q + \alpha = 2$ . The concentration profile found from the simulation results has exactly this form with  $\lambda = 2$ .

On the other hand, the velocity field is related to the concentration through Darcy's law (see e.g. [14]) which can be written as

$$\nabla \times [\beta(C) \mathbf{v}] = 0, \quad (4)$$

or

$$R(\mathbf{v} \times \nabla C) + (\nabla \times \mathbf{v}) = 0, \quad (5)$$

with  $R = \partial \ln \beta / \partial C$ , where  $\beta$  is the damping function which, in the fingering simulations, controls the drag and depends on the concentration  $C(x)$ . The solution to Eq.(5) is a function  $\mathbf{v}(C)$  which, through the concentration, is space dependent, but is analytically unknown. However, given that the concentration

exhibits a  $q$ -Gaussian profile (3), one can expect that the velocity field also assumes a  $q$ -Gaussian form. For the transverse velocity field, Fig.2b shows that the  $q$ -Gaussian interpretation is in perfect agreement with the data obtained from the simulation results, i.e.

$$v_x(x) = v_0 [1 - (1 - q)\phi_q x^2]^{\frac{1}{1-q}}, \quad (6)$$

where  $v_0$  is a normalization constant. Note that the value of  $q$  in (6) is not the same as in (3). So the pattern of alternating vortices of the transverse velocity amplitude as seen in Fig.2a can be viewed as a landscape of hills and wells of radial  $q$ -Gaussians distributed along the concentration profile of the interfacial zone.

We next consider the velocity distribution which follows from this spatial profile. The  $q$ -Gaussian spatial profile (shown in Fig.2b) is obtained experimentally by measuring the  $v_x$  amplitude in a section plane orthogonal to the  $y$ -axis. Now each  $q$ -Gaussian "blob" in Fig.2a is a function of  $r^2 = x^2 + y^2$  and is expected to be radially symmetric. So generalizing the  $q$ -exponential in Eq.(6) to an arbitrary power  $\lambda$  of the radial variable  $r$ , we have

$$v(r) \equiv v_x(r)/v_0 = e_q^{-\phi_q r^\lambda} = [1 - (1 - q)\phi_q r^\lambda]^{\frac{1}{1-q}}, \quad (7)$$

We seek to establish the corresponding probability distribution function  $P(v)$  which, for the sake of generality, is considered in  $d$  dimensions

$$P(v) = c_d \int_0^\infty r^{d-1} |dr| \delta(v(r) - v), \quad (8)$$

where  $c_d$  is an integration constant. Expression (7) is inverted to give  $r^\lambda = -\frac{1}{\phi_q} \ln_q v$  which is used in (8) to obtain

$$P(v) = c_d \frac{|r|^{d-\lambda} v^{-q}}{\lambda \phi_q} = \frac{c_d}{\lambda \phi_q^{d/\lambda}} [-\ln_q v]^{\frac{d-\lambda}{\lambda}} v^{-q}. \quad (9)$$

For two-dimensional systems ( $d = 2$ ) with  $q$ -Gaussian spatial profile ( $\lambda = 2$ ), we obtain the power law distribution

$$P(v) = \frac{c_d}{\phi_q} v^{-q}. \quad (10)$$

This is exactly the power law that we find for the transverse velocity distribution as exhibited in Fig.3 where a fit to the simulation data gives an exponent  $q < 1$  (indicating statistical importance of large values of the velocity).

In conclusion, we have presented an analysis and an interpretation of the statistical behavior of the transverse velocity field in the "onset" region of the fingering process just below the dynamical transition. To the best of our knowledge, this transition has remained unexplained analytically. The velocity distribution analysis developed in the present paper offers a method to investigate both the transverse and longitudinal velocity fields,  $P(v_x)$  and  $P(v_y)$  respectively, below and above the dynamical transition, and should therefore provide insight in the nature of the transition as will be discussed elsewhere.

## Acknowledgements

This work was supported by a grant from the *European Space Agency* and *PRODEX* (Belgium) under contract ESA/14556/00/NL/SFe(IC).

## References

- [1] C. Beck, G.S. Lewis, and H. L. Swinney, *Phys. Rev.E* (2001) **63**, 035303(R).
- [2] C. Beck, *Phys. Rev. Lett.* (2001) **87**, 180601.
- [3] C. Tsallis, *Physica D* (2004) **193**, 3.
- [4] P. Grosfils and J.P. Boon, *J. Mod. Phys. B* (2003) **17**, 15 .
- [5] See e.g. J. Bear, *Dynamics of Fluids in Porous Media* (Dover, New York, 1988).
- [6] S. Succi, *The Lattice Boltzmann Equation for Fluid Dynamics and Beyond* (Clarendon Press, Oxford, 2001).
- [7] E.G. Flekkoy, U. Oxaal, J. Feder, and T. Jossang, *Phys. Rev.E* (1995) **52**, 4952.
- [8] P. Grosfils, J.P. Boon, J. Chin, and E.S. Boek, *Phil. Trans. Royal Soc.* (2004) **362**, 1723.
- [9] C. Tsallis and D.J. Bukman, *Phys. Rev.E* (1996) **54**, R2197.
- [10] L. Borland, *Phys. Lett. A* (1998) **245**, 67; *Phys. Rev.E* (1998) **57**, 6634.
- [11] L.C. Malacarne, R.S. Mendes, I.T. Pedron, and E.K. Lenzi, *Phys. Rev.E* (2001) **63**, 030101R.
- [12] I.T. Pedron, R.S. Mendes, L.C. Malacarne, and E.K. Lenzi, *Phys. Rev.E* (2002) **65**, 0411108.
- [13] A. Compte and D. Jou, *J. Phys. A: Math. Gen.* (1996) **29**, 4321.
- [14] G.M. Homsy, *Ann. Rev. Fluid Mech.* (1987) **19**, 271.

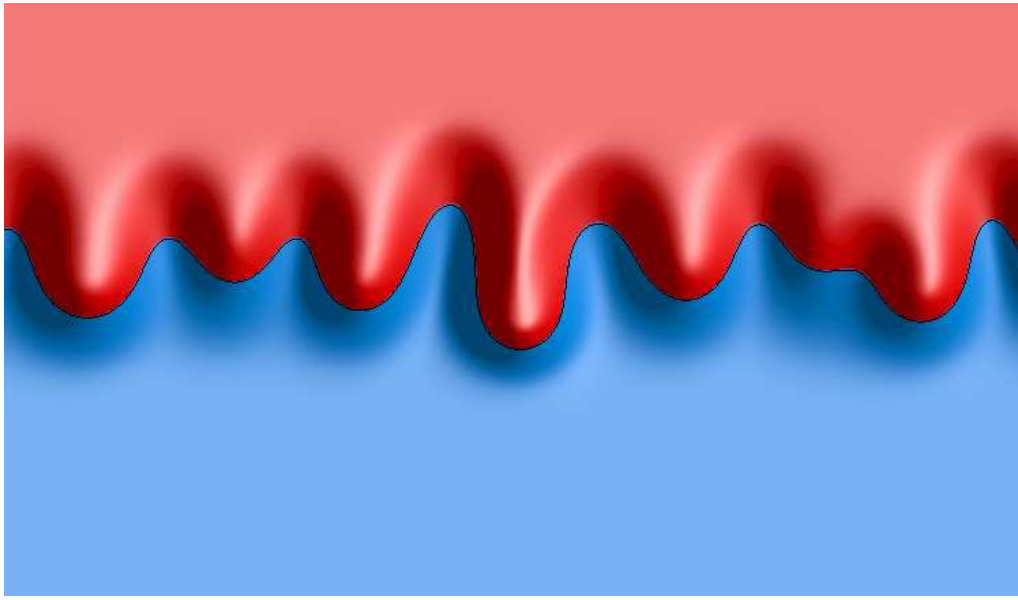


Fig. 1. Illustration of Lattice Boltzmann (BGK) simulation of viscous fingering. The mixing length between the two fluids is clearly identified by the shadow zone around the density ( $= 0.5$ ) isoline (color code indicating the concentration of the invading fluid from red ( $C_1 = 1$ ) to blue ( $C_1 = 0$ )).

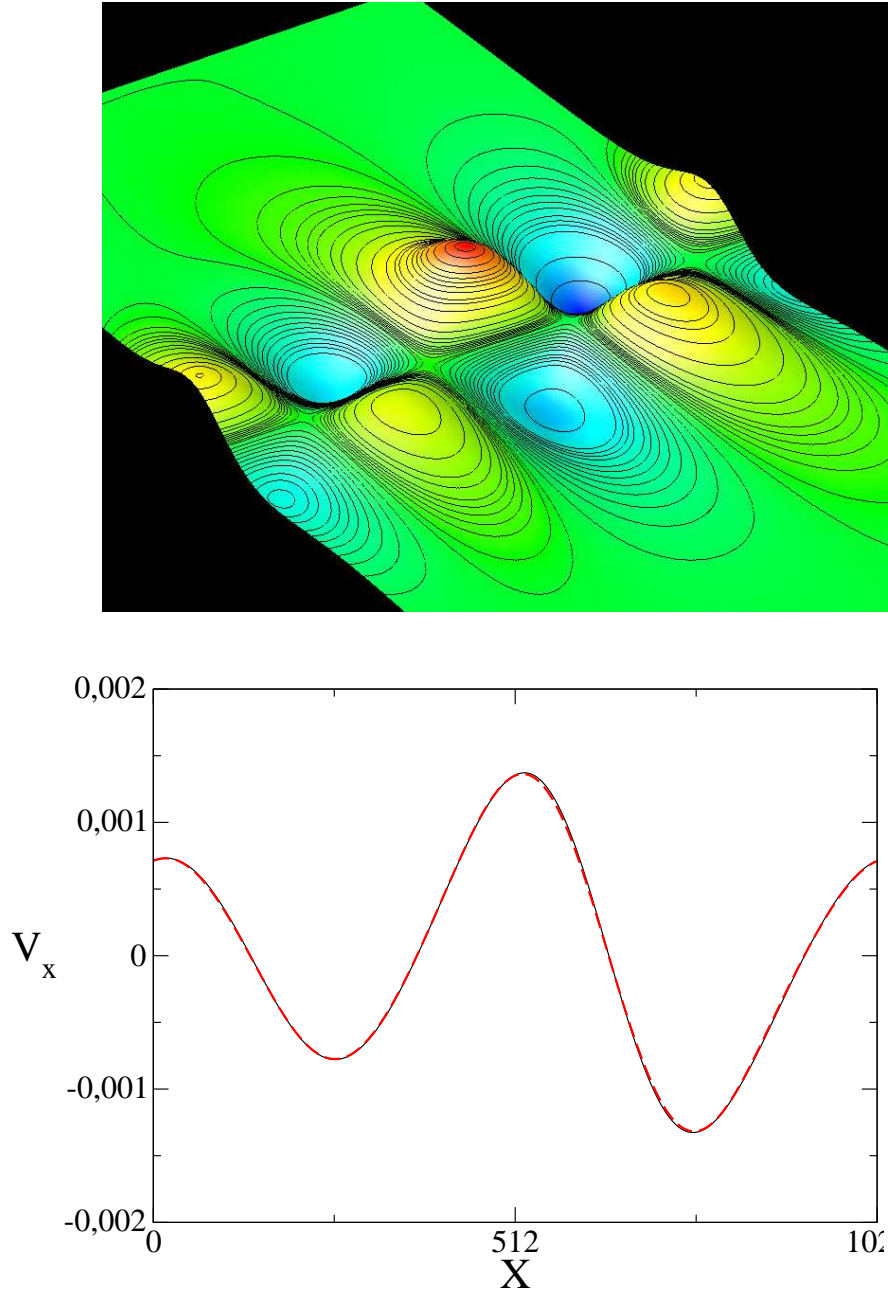


Fig. 2. (a) Upper panel: Transverse velocity field showing landscape of  $q$ -Gaussian "hills and wells"; simulation data with iso-velocity contours, color code indicating highest positive values (red) to largest negative values (blue) of  $v_x$ . (b) Lower panel: Transverse velocity profile (solid line) obtained from the simulation data by a section plane cut through the hills and wells parallel to and North-West of the main valley in the upper panel; analytical function Eq.(6) (dashed line): the convex and concave curves are connected by summation of  $q$ -Gaussians.

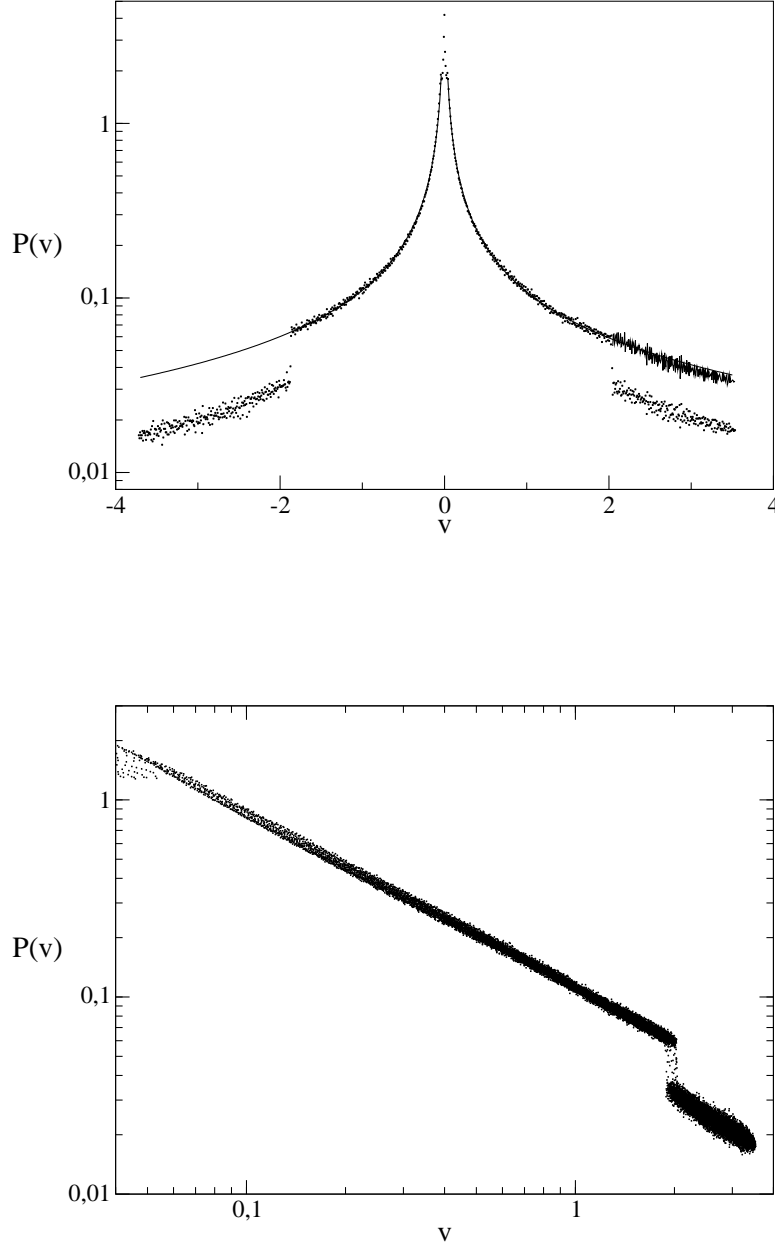


Fig. 3. Velocity distribution with power law fit :  $P(v)$  with  $v = (v_x - \langle v_x \rangle) \sigma^{-1}$  where  $\langle v_x \rangle$  is the mean transverse velocity and  $\sigma = [\langle v_x^2 \rangle - \langle v_x \rangle^2]^{1/2}$ . Data are rescaled (shifted upwards in the far right branch of the upper panel) showing that all data follow the same power law down to values  $v \simeq 0.05$  (below which statistics become insufficient; here 5 points with  $v < 0.05$  out of 1000).  $P(v) = A|v|^{-q}$  (Eq.(10)) with  $q = 0.8739$  and  $A = 0.1082$  for  $|v| > 0$ , and  $q = 0.8787$  and  $A = 0.1054$  for  $|v| < 0$ . Lower panel illustrates power law for 40 sets of data taken at successive times.